JOURNAL OF THERMOPHYSICS AND HEAT TRANSFER
Vol. 10, No. 3, July–September 1996

Acceleration Schemes for the Discrete Ordinates Method

W. A. Fiveland* and J. P. Jessee†
Babcock and Wilcox, Alliance, Ohio 44601

Discrete ordinates (DO) methods have been developed to solve the multidimensional radiative transport equation (RTE) for applications including combustion processes and other combined-mode heat transfer cases. The convergence of DO methods is known to degrade for optical thicknesses greater than unity, which occur for example in a flame. Acceleration schemes have been developed for use in neutron transport applications, but little work has been done to accelerate convergence of the RTE for radiative heat transfer applications. This article presents several acceleration schemes for the RTE, including successive overrelaxation, synthetic acceleration, and mesh rebalance methods. Solution convergence is discussed and demonstrated using two- and three-dimensional examples. Although all methods improve convergence, the mesh rebalance method improves the RTE convergence best. For some conditions, the rebalance method improves convergence dramatically, reducing RTE iterations by an order of magnitude. However, the mesh rebalance method fails to produce convergence of the RTE for large optical thicknesses and fine mesh discretizations. Examples are used to demonstrate that improved convergence can be obtained by solving the rebalance equation on a coarser grid, which is determined by regrouping the base RTE grid, until an optical thickness of near unity is obtained on the coarse grid. Based on these findings, a general solution strategy is discussed.

Nomenclature

A = area, m^2
a = finite volume coefficients
f = correction factor
G = incident energy, W/m^2
I = intensity, W/m^2-sr
L = length of domain, m
M = total number of discrete ordinates directions
N_b = number of neighbor nodes
N_D = number of space dimensions
n = inward facing surface normal
q = heat flux, W/m^2
R = residual norm
r = position vector, m
S = source term, W/m^3-sr
S_n = order of discrete ordinates approximation
V = volume, m^3
w_k = direction weights
x, y, z = spatial coordinates, m
α = relaxation factor
β = extinction coefficient, $\kappa + \sigma$, m^{-1}
Γ = operator
ε = emissivity
κ = absorption coefficient, m^{-1}
Λ = operator
μ, ξ, η = direction cosines
ρ = reflectivity, $1 - \varepsilon$
σ = scattering coefficient, m^{-1}
τ = optical thickness
Ω = direction with direction cosines, μ, ξ, η
ω = albedo, σ/β

Subscripts
b = blackbody
e = emission
j = control volume index
k = generic summation index
L = local
l = lower-order
m = direction
n = nth S_n approximation
p = central control volume index
s = in-scattering

Superscripts
i = iteration
p = predicted value
$'$ = incoming direction
$\hat{}$ = unit vector
out = outgoing
in = incoming

Received May 15, 1995; revision received Dec. 8, 1995; accepted for publication Jan. 12, 1996.

*Manager, Numerical Modeling Section, Research and Development Division, 1562 Beeson Street. Member AIAA.

†Research Engineer, Numerical Modeling Section, Research and Development Division, 1562 Beeson Street.

Introduction

In many combustion devices, such as furnaces and burners, radiant heat transfer is the dominant mode of heat transfer and significantly affects the gas and wall temperature distributions. Because reaction rates and density distributions are closely linked to the local gas temperatures, radiation heat transfer plays a large role in governing the combustion dynamics. As a consequence, accurate prediction of the performance of practical combustion devices requires robustly converging methods for solving the radiative transport equation.

During the last two decades, considerable attention has been focused on developing solutions of the radiative transport equation (RTE) applicable to multidimensional geometries. The relative merits of the various methods have been extensively reviewed elsewhere.[1,2] Of these methods, the discrete ordinates (DO) method has received widespread use for practical problems.[3–8]

In the DO method, the RTE is generally solved iteratively. The contribution of in-scattering is determined with intensities from the previous iteration. The basic DO method is known to converge very slowly as the optical thickness increases.[2,9] Some applications, including the combustion of fossil fuels, locally produce optically thick conditions in the flame that inhibit DO convergence, often rendering the method impractical. In addition, if spectral effects are considered and a band

method[10] is applied, a DO strategy is required that is robust. Discrete ordinates solution methods have been extensively developed for the neutron transport process. For those applications, methods have been developed to accelerate the neutron transport equation, and a review of these acceleration methods has been presented.[9] In contrast, little work has focused on accelerating solutions of the RTE, except the recent work of Chui and Raithby,[11] in which a mesh rebalance-like equation was solved implicitly with the RTE.

This article presents several methods of accelerating the convergence of the RTE. These methods include successive overrelaxation, mesh rebalance, and synthetic acceleration methods. Solution convergence is discussed and demonstrated using simple examples in two and three dimensions. The rebalance method is shown to converge best, but it fails to produce convergence of the RTE for some conditions. An improved strategy is proposed for solving the RTE with mesh rebalance that yields a robust DO method. A necessary criterion to achieve convergence is introduced and demonstrated.

Technical Approach

Discrete Ordinates Method

The discrete ordinates method is a general method for solving the neutron or radiative transport equations. Originally, the discrete ordinates method was proposed by Chandrasekhar,[12] and was later developed for neutron transport applications by Lathrop and Carlson.[13] Subsequently, the method was developed for radiative heat transfer.[3-8] For simplicity, this article considers gray properties and isotropic scattering. However, the presented acceleration methods should apply for nongray conditions and anisotropic scattering.

The general radiative transport equation for a participating media may be derived by considering the balance of energy passing in a specified direction $\boldsymbol{\Omega}$ through a differential volume, as shown in Fig. 1. For an emitting–absorbing and isotropically scattering medium, the RTE is

$$(\boldsymbol{\Omega}\cdot\nabla)I(\boldsymbol{r}, \boldsymbol{\Omega}) = -(\kappa + \sigma)I(\boldsymbol{r}, \boldsymbol{\Omega}) + \frac{\sigma}{4\pi}\int_{4\pi} I(\boldsymbol{r}, \boldsymbol{\Omega}')\, \mathrm{d}\Omega' + \kappa I_b(\boldsymbol{r}) \tag{1}$$

where $I(\boldsymbol{r}, \boldsymbol{\Omega})$ is the radiation intensity, which is a function of position and direction; and $I_b(\boldsymbol{r})$ is the intensity of blackbody radiation at the temperature of the medium.

If the surface is assumed to emit and reflect diffusely, then the radiative boundary condition for Eq. (1) is given by

$$I(\boldsymbol{r}, \boldsymbol{\Omega}) = \varepsilon I_b(\boldsymbol{r}) + \frac{\rho}{\pi}\int_{\hat{\boldsymbol{n}}\cdot\boldsymbol{\Omega}'<0} |\hat{\boldsymbol{n}}\cdot\boldsymbol{\Omega}'|\, I(\boldsymbol{r}, \boldsymbol{\Omega}')\, \mathrm{d}\Omega' \tag{2}$$

where Eq. (2) applies for $\boldsymbol{\Omega}\cdot\hat{\boldsymbol{n}} > 0$. $I(\boldsymbol{r}, \boldsymbol{\Omega})$ is the intensity leaving a surface at a boundary condition location, ε is the surface emissivity, ρ is the surface reflectivity, and $\hat{\boldsymbol{n}}$ is the unit normal vector at the boundary location. Equations (1) and (2) represent the governing equation and boundary conditions, respectively, for radiative heat transfer.

The numerical solution of the RTE requires discretization of both angular and spatial domains. Formally, the discrete ordinates method only pertains to the angular discretization. In the discrete ordinates method, the governing RTE is replaced by a discrete set of equations for a finite number of directions $\boldsymbol{\Omega}_m$, and each integral is replaced by a quadrature:

$$(\boldsymbol{\Omega}_m\cdot\nabla)I(\boldsymbol{r}, \boldsymbol{\Omega}_m) = -\beta I(\boldsymbol{r}, \boldsymbol{\Omega}_m) + \frac{\sigma}{4\pi}\sum_{k=1}^{M} w_k I(\boldsymbol{r}, \boldsymbol{\Omega}_k) + \kappa I_b \tag{3}$$

This angular approximation transforms the original integrodifferential equation into a set of coupled differential equations. Commonly, the weights and directions are based on the S_n approximation,[4,5] which has $n(n + 2)$ discrete directions. Spatial discretization has been accomplished using a number of variations of the finite volume method.[3-5,14-16]

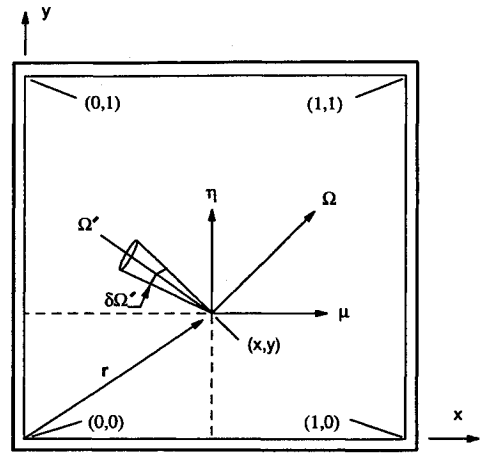

Fig. 1 Geometry for case 1.

Iterative Solution Algorithm

Equation (3) is usually solved with an iterative algorithm as follows:

$$\Gamma_m I_m^{i+1} = S_{s,m}(I^i) + S_e \tag{4}$$

where the operator Γ_m can be written

$$\Gamma_m = (\boldsymbol{\Omega}_m\cdot\nabla) + \beta \tag{5}$$

and the terms on the right-hand side of Eq. (4) are the in-scattering and emission source terms, respectively.

With an initial guess for the sources, the transport equation for each ordinate direction is discretized and solved independently.[3] When the intensities in the domain have been calculated for each of the directions, sources are updated using these intensities. One global iteration is defined by a complete sweep through the space–angle mesh. Global iterations are performed until convergence is obtained.

With an acceleration scheme, an additional step is introduced. The transport equation is solved to produce a field of predicted intensities:

$$\Gamma_m I_m^{p,i+1} = S_{s,m}(I^i) + S_e \tag{6}$$

These intensities are used to determine predicted estimates of the sources, $S_{s,m}^{p,i+1}$. An acceleration scheme is subsequently used to correct the in-scattering source to obtain $S_{s,m}(I^{i+1})$. One advantage of segmenting the solution into predictor/corrector steps is to facilitate examining a variety of acceleration methods.

Acceleration Methods

Acceleration schemes have been developed for the neutron transport equation and include Chebyshev acceleration,[17] mesh rebalance methods,[18,19] and synthetic acceleration methods.[19,20] Lewis and Miller[9] have reviewed the methods as applied to neutron transport applications. Little work has been done for radiative applications, other than the work of Chui and Raithby.[11]

Successive Overrelaxation

A simple method is successive overrelaxation (SOR) in which the in-scattering source is advanced by

$$S_m^{i+1} = S_m^i + \alpha(S_m^{p,i+1} - S_m^i) \tag{7}$$

where α is the overrelaxation factor and is contained in the interval $1 < \alpha < 2$.

Mesh Rebalance

The mesh rebalance method can be formulated using Eq. (3) summed over all of the ordinate directions:

$$\nabla \cdot q(r) + \kappa G(r) = 4\pi\kappa I_b \tag{8}$$

This transport equation contains the net flux and incident energy defined by

$$q = \int_{4\pi} I(r, \Omega)\Omega \, d\Omega = \sum_{k=1}^{M} w_k \Omega_k I(r, \Omega_k) \tag{9}$$

$$G = \int_{4\pi} I \, d\Omega = \sum_{k=1}^{M} w_k I(r, \Omega_k) \tag{10}$$

A control volume form of Eq. (8) can be written as

$$\sum_{k=1}^{N_b} q_k A_k + \kappa G_j V_j = 4\pi\kappa I_{b,j} V_j \tag{11}$$

where the q_k are the net fluxes out of the control volume at face locations:

$$q_k = q_k^{\text{out}} - q_k^{\text{in}} = \int_{n \cdot \Omega' < 0} I_k(r, \Omega)\Omega \, d\Omega - \int_{n \cdot \Omega' > 0} I_k(r, \Omega)\Omega \, d\Omega \tag{12}$$

The values q_k^{out} and q_k^{in} denote the directional fluxes out of and into the control volume, respectively.

Mesh rebalance associates a correction factor f_j for each subvolume V_j:

$$I_j^{i+1} = f_j I_j^{p,i+1} \tag{13}$$

For the simplest case, base mesh rebalance (BMR), one factor is applied to each volume; however, factors may also be applied to coarser grids and/or coarser finite solid angles. The base mesh rebalance method is also known as the fine mesh rebalance method.[19] With Eqs. (12) and (13), the fluxes in Eq. (11) are rewritten. Assuming a first-order upstream dependence, the outgoing flux is influenced by the factor f_j, whereas the incoming flux is influenced by the factor from the corresponding neighbor volume. This leads to a transport equation in local indices:

$$a_p f_p = \sum_{k=1}^{N_b} a_k f_k + b \tag{14}$$

with the coefficients for three-dimensional applications given by

$$a_p = \sum_{k=1}^{N_b} q_k^{\text{out}} A_k + \kappa G_p V_p \tag{15}$$

$$a_k = q_k^{\text{in}} A_k \tag{16}$$

$$b = 4\pi\kappa I_{b,p} V_p \tag{17}$$

At the boundaries, the discrete transport equation adjacent to the surface is modified. The product of surface reflectance, incoming heat flux, and area is subtracted from Eq. (15), whereas the product of the surface emittance, emissive power, and area is added to the source term, Eq. (17). The system of equations [Eq. (14)] is solved and sources are updated using Eq. (13). The effect of the mesh rebalance method is to adjust the average amplitude of the in-scattering source term in each control volume to satisfy conservation of radiant energy.

Synthetic Acceleration

Another approach to accelerate the RTE is the technique of synthetic acceleration,[9] in which the RTE is integrated over all directions Ω, to obtain

$$\int_{4\pi} \Lambda I \, d\Omega = \int_{4\pi} S_e \, d\Omega \tag{18}$$

where the operator is defined, $\Lambda = \Gamma - \sigma$. A low-order operator Γ_l is introduced to produce

$$\int_{4\pi} (\Gamma_l + \Lambda - \Gamma_l) I \, d\Omega = \int_{4\pi} S_e \, d\Omega \tag{19}$$

Equation (19) may be rearranged into the following form:

$$\int_{4\pi} \Gamma_l I \, d\Omega = \int_{4\pi} S_e \, d\Omega - \int_{4\pi} (\Lambda - \Gamma_l) I \, d\Omega \tag{20}$$

This suggests the iterative scheme

$$\int_{4\pi} \Gamma_l I^{i+1} \, d\Omega = \int_{4\pi} S_e^i \, d\Omega - \int_{4\pi} \Lambda I^{p,i+1} \, d\Omega + \int_{4\pi} \Gamma_l I^{p,i+1} \, d\Omega \tag{21}$$

Since Γ_l is independent of Ω, and using Eq. (18), it follows

$$\Gamma_l (G^{i+1} - G^{p,i+1}) = \int_{4\pi} \Lambda (I^i - I^{p,i+1}) \, d\Omega \tag{22}$$

and finally,

$$\Gamma_l (G^{i+1} - G^{p,i+1}) = \sigma (G^{p,i+1} - G^i) \tag{23}$$

The low-order operator Γ_l was chosen to be the P1-approximation[2] defined by

$$\Gamma_l = -\nabla \cdot D\nabla + \kappa \tag{24}$$

with a diffusion coefficient D of units to maintain stability. The spatially discrete form of Eq. (23) is a symmetric system and can be solved with any standard equation solver.

Discussion

The basic discrete ordinates method of Fiveland[3,4] with a first-order accurate step approximation was used, since the method is unconditionally stable, producing only positive intensities. Therefore, any nonconverging solution is a consequence of in-scattering source terms not approaching a limit. Convergence is defined when the normalized incident energy residual decreases below 10^{-5}:

$$R^{i+1} = \left\| \frac{G^{i+1} - G^i}{G^i} \right\|_\infty < 1 \times 10^{-5} \tag{25}$$

For isotropic scattering and black walls, this residual is directly related to the transport residual, and its approach to zero is both a necessary and sufficient condition for convergence of the DO equations. Unless otherwise indicated, the S_4 ordinate set was used for all cases. Solutions were initiated by assuming the in-scattering source terms were zero.

Some computational overhead is required over the standard DO calculations for each of the acceleration schemes. The overhead for rebalance and synthetic acceleration schemes results from the formation and solution of the discrete rebalance and diffusion equations. These systems of discrete equations

are linear, and the corresponding matrices are usually M matrices,[17] for which good smoothing methods may be found. Iterative solvers based on multigrid theory are generally most effective in solving these linear equations. When applied to elliptic systems, the computational work for multigrid solvers scales linearly with problem size. Since the work for the base DO calculations per iteration also scales linearly with problem size, the percentage of overhead should be largely independent of spatial discretization. In addition, computational work for the multigrid solution of the rebalance and diffusion equations should be a fraction of the work required for standard DO calculations. Because this article is concerned with gross convergence improvements, convergence comparisons are based primarily on the number of global iterations through the space-angle mesh. However, to illustrate the realized efficiency gain and to prove the hypothesis of fractional overhead, CPU times with and without rebalance are given later for one of the cases.

Basic Acceleration Schemes

The convergence characteristics of the discrete ordinates method were studied for several enclosures. Case 1 considers radiative heat transfer in a two-dimensional, rectangular enclosure ($x/L = 1$, $y/L = 1$) with a purely scattering and cold medium, enclosed by black and cold walls, except for the wall at $y = 0$, which has an emissive power of unity.[3,21] The geometry is shown in Fig. 1.

Figure 2 presents the convergence characteristics of case 1 for several acceleration methods over a wide range of optical thicknesses. Results are presented using a 5 × 5 discretization of the RTE. The BMR method clearly indicates improved convergence over the entire range of scattering coefficients. This is somewhat surprising, since the neutron literature[19,20] indicates the synthetic acceleration should have more promise. However, the RTE has more complex boundary conditions that could affect the convergence history. The improvements in RTE convergence using BMR might suggest the rebalance method is as effective for any discretization of the RTE. This is not the case, as shown later.

The results shown in Fig. 2 for the BMR method are very similar to those presented by Chui and Raithby[11] using their implicit acceleration method. This is not surprising since this implicit method is conceptually identical to the BMR scheme of Reed.[19] In addition, both schemes may be interpreted as non-Galerkin projection methods (see also Ref. 19).

Table 1 lists the iterations required for convergence of the case 1 geometry, using a 5 × 5 mesh and the SOR method. For optical thicknesses τ of two or below, an optimal relaxation factor exists that produces near-rebalance performance, although not quite as good. As optical thicknesses increase, the DO method converges very poorly with SOR compared to base mesh rebalance.

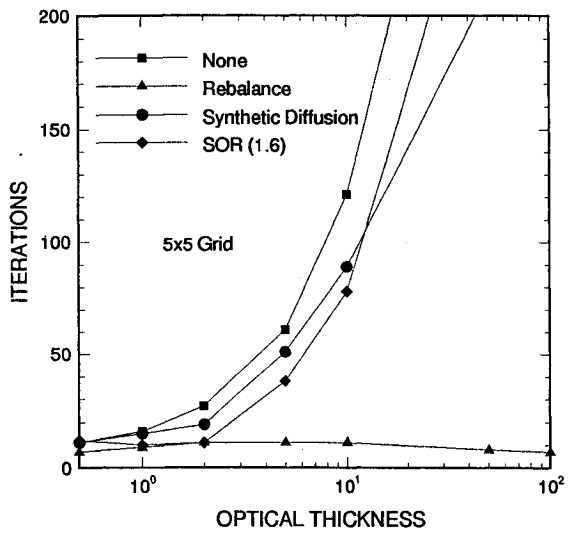

Fig. 2 Iterations required for convergence of case 1 (two-dimensional geometry).

Table 1 Iterations required for convergence of case 1 with SOR and a 5 × 5 grid

	$\tau = \sigma L$					
α	0.5	1.0	2.0	5	10	20
1.0	11	16	27	61	121	243
1.2	8	13	22	51	102	206
1.4	9	10	18	44	89	179
1.6	12	10	16	38	78	159
1.8	20	15	13	34	70	143
2.0	44	25	15	31	63	129

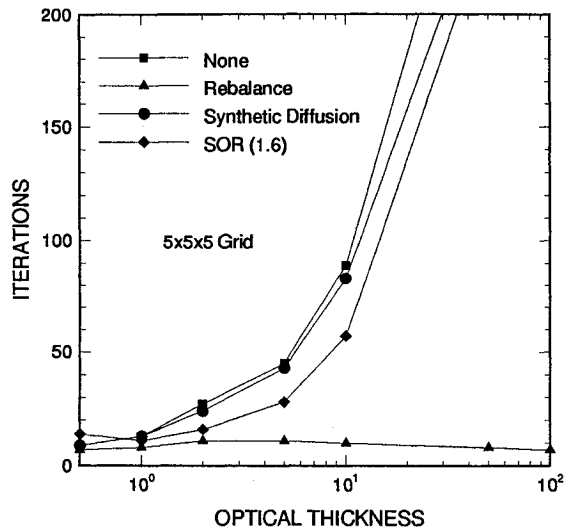

Fig. 3 Iterations required for convergence of case 2 (three-dimensional geometry).

With the radiative conditions and geometry of case 1 as a basis, the convergence characteristics of the DO method were examined for a range of scattering albedos ω from 0.1 to 1.0. The limit of an albedo of zero was not studied, since convergence of the RTE can be found in a single iteration and an acceleration scheme is not needed. The basic DO method with synthetic acceleration and successive overrelaxation methods converges better as the albedo decreases, but the number of iterations for convergence is still unsatisfactory, 100 iterations or more to converge for many optical conditions. The BMR method consistently converges the RTE in less than 10 or 11 iterations for the range of albedo studied.

In case 2, convergence characteristics were studied for a three-dimensional enclosure ($x/L = 1$, $y/L = 1$, $z/L = 1$), with a cold, purely scattering medium, surrounded by radiatively black and cold walls, except for the wall at $y = 0$, which has an emissive power of unity. Figure 3 presents the convergence characteristics of case 2 for several acceleration methods over a wide range of scattering coefficients. Results are presented using a 5 × 5 × 5 discretization of the RTE. The results are similar to case 1. The rebalance method shows the best convergence and generally exhibits improved convergence over the entire range of optical thicknesses.

Because the mesh rebalance method shows promise over the range of optical thickness encountered in many RTE applications, the remaining discussion is focused on that method. To investigate the scaling efficiency of the BMR method, case 1 was reanalyzed with spatial discretizations ranging from 4 × 4 to 100 × 100. The iterations required for convergence are presented in Fig. 4. The results indicate that for coarse discretizations, good convergence can be achieved for a wide

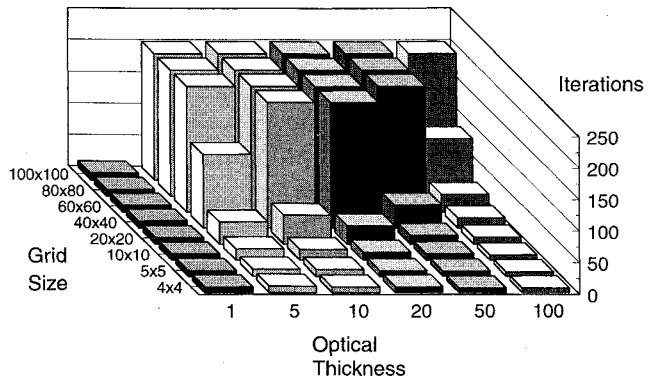

Fig. 4 Iterations for convergence of case 1 with base mesh rebalance. (Iterations above 200 are not shown.)

range of optical properties. However, the rebalance method fails as the discretization becomes finer and the optical thickness is above unity. The problems in converging the RTE as the scattering coefficient increases are well known, since there is loss of the spatial derivative in singular perturbation parlance.[22] The results are perplexing; fine meshes are needed to obtain solution accuracy, but at the same time, these meshes destroy the utility of the rebalance method. An alternative mesh rebalance scheme is now proposed.

Coarse Mesh Rebalance Scheme

In an attempt to improve convergence for fine spatial discretization, the coarse mesh rebalance (CMR) method is applied. The method is identical to the BMR method, except that a coarser mesh is used for the rebalance equation than for the RTE. This approach is an attempt to average the components of the error in the source term of the RTE over a larger spatial region.

The influence of the CMR scheme for case 1 is displayed in Figs. 5a and 5b. Results are shown for optical thicknesses of 10 and 20 and RTE grids ranging from 20 × 20 to 100 × 100. For each RTE grid, a variety of rebalance meshes are considered. The rebalance meshes are obtained by grouping the volumes of the RTE grid in blocks of 1 × 1 to 10 × 10. The 1 × 1 grouping corresponds to the base mesh rebalance scheme. Surprisingly, the best convergence does not always occur for the BMR method (i.e., rebalance on the base grid). One interesting feature of Figs. 5a and 5b is that the best convergence is obtained for an RTE discretization when the rebalance grouping produces a local optical thickness near unity; e.g., 20 × 20 RTE grid, σ of 10, and rebalance grouping of 2 × 2 yielding $\tau_L = 0.05(10)2 = 1$. Figure 6 shows the rate of convergence for several different rebalance grids. The maximum rate of convergence clearly occurs when the local optical thickness is near unity. This leads next to a strategy to achieve optimum convergence for a set of optical properties.

Adaptive Rebalance Scheme

As observed in Figs. 5a and 5b, the effectiveness of the mesh rebalance method is largely dependent on the grid size, global optical thickness, and coarseness of the rebalance mesh. From an empirical viewpoint, the success of the method may be correlated against the local optical thickness of the rebalance mesh as shown in Fig. 7. The optimal rebalance mesh has a local or cell optical thickness slightly above unity. Little guidance, either theoretically or empirically, has been given in literature for the selection of the optimal rebalance mesh.

The theoretical explanation for the previous observations may be found in the field of multigrid or multilevel methods. These methods differ from conventional methods, because they resolve different components of error in the iterative solution

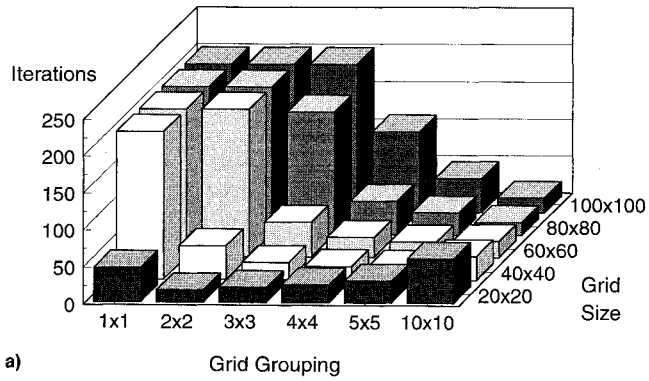

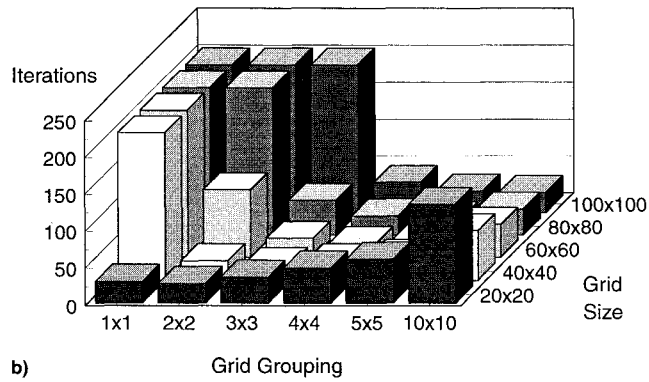

Fig. 5 Iterations required for convergence of case 1 with coarse mesh rebalance method. τ = a) 10 and b) 20. (Iterations above 200 are not shown.)

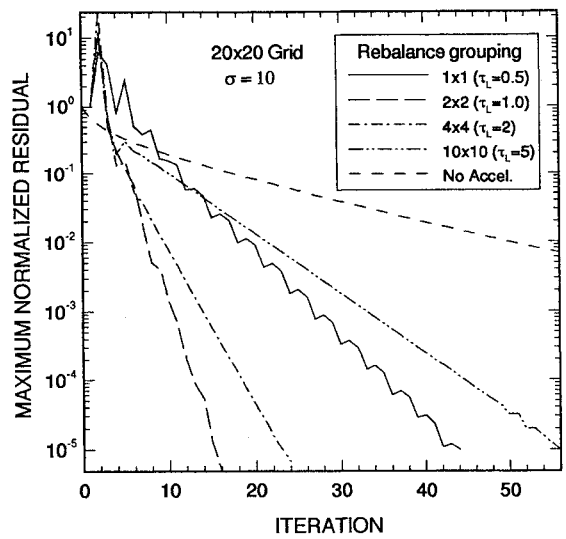

Fig. 6 Rebalance convergence history of case 1 for several coarse meshes.

by using a variety of computational levels or grids. High-frequency error is resolved using a fine grid, whereas low-frequency error is resolved using a coarse grid. The detailed theory is beyond the scope of this article, but may be found in Refs. 23–26.

Interestingly, the mesh rebalance method may be considered a member of the general family of multilevel methods, although the advent of the mesh rebalance method predates the pioneering multigrid work of Brandt[23] by over a decade. The BMR method corresponds to a two-level multigrid scheme: 1) the fine grid corresponding to the standard space–angle mesh, and 2) the coarse grid corresponding to the base spatial mesh

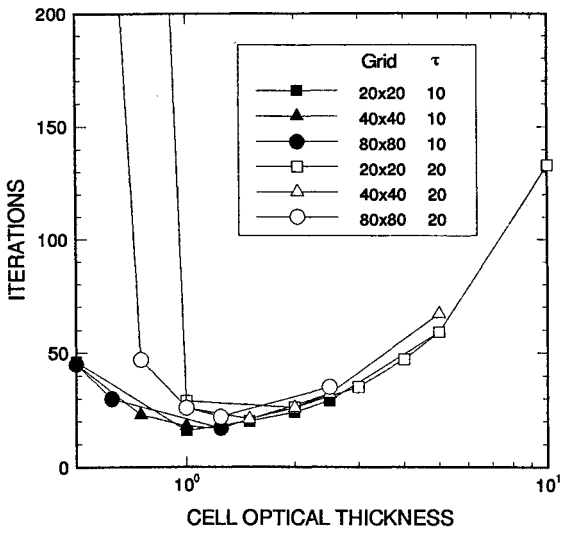

Fig. 7 Rebalance convergence correlated with cell optical thickness.

and a collapsed angular mesh. The angular coarsening reduces M degrees of freedom per control volume to just one. This differs from the standard multigrid concept: the angular rather than the spatial discretization is coarsened.

The effectiveness of the BMR method for local optical thicknesses greater than unity may be explained from a multigrid perspective. For these cases, the in-scattering terms are dominant in the discrete equations: the angular coupling is stronger than the spatial coupling. Consequently, the standard block iterative solution procedure that individually considers each direction converges slowly because of the inability to resolve spatial error (here, error indicates the difference between the current estimate and the final numerical solution). The solution propagates slowly across the spatial mesh because of the dominance of the explicitly treated in-scattering source terms. The BMR method accelerates the solution by effectively propagating the solution across the domain, resolving all components of spatial error. The angular error is effectively resolved using the standard sweeping scheme[3,4] for the discrete RTE through the complete space–angle mesh.

As noted in Fig. 4, the effectiveness of the BMR scheme degrades as the cell optical thickness decreases (e.g., when the spatial grid is refined). For coarse base meshes, the local optical thickness is large, and the rebalance method is effective as described in the previous paragraph. However, for finer meshes, the local optical thickness is relatively small, even though the global optical thickness is large. The local spatial coupling is stronger than the angular coupling. Consequently, the basic sweeping procedure of the discrete RTE through the space–angle mesh is effective in resolving high and moderate frequency spatial error, but still cannot extinguish low-frequency spatial error. The BMR method attempts to resolve this low-frequency spatial error. Unfortunately, the rebalance overly corrects the solution, destroying the local balances obtained with the basic sweeping scheme for the discrete RTE through the space–angle mesh.

The previous problem for fine meshes is circumvented by resorting to a CMR scheme in which blocks of control volumes are corrected together. The CMR scheme effectively removes the low-frequency spatial error, while leaving the local balances basically untouched. Angular and high and moderate frequency spatial errors are resolved using the basic sweeping scheme for the discrete RTE.

The previous discussion suggests that the optimal rebalance method should be based on a coarse mesh that removes components of error with spatial frequencies lower than those that may be removed via the basic sweeping process. Empirically, such a coarse mesh was found to yield a local optical thickness of slightly above unity. Theoretically, the value of unity represents a balance between spatial and angular coupling. An automated scheme was devised to select the coarse mesh such that the coarse volumes have optical thicknesses between 1 and 2. The optical thickness of a coarse volume was defined as

$$\tau_L = 2N_D \left(\int_V \sigma \, dV \Big/ \oint_S dS \right) \tag{26}$$

where the integrals are over the volume and surface area of the coarse volumes, respectively, and N_D is the dimension of the problem (2 for two-dimensional and 3 for three-dimensional). In the implementation, fine volumes were added to a coarse volume until Eq. (26) was greater than 1.

To test the adaptive rebalance scheme, case 1 was revisited for a number of scattering coefficients and grid discretizations. Convergence results are shown in Fig. 8. As seen in this figure, the adaptive scheme effectively accelerates convergence for the entire range of global optical thickness and spatial discretizations. These results contrast the unreliable convergence of the BMR method as shown in Fig. 4. Although this is a fairly simple example (uniform grid and homogeneous properties), it illustrates the utility of the adaptive rebalance scheme.

For practical combustion problems, optical properties are generally nonhomogeneous and cell aspect ratios may become large. The previous adaptive scheme should greatly increase the robustness of standard solution process; but nevertheless, refinements in the adaptive scheme may be required to provide excellent performance displayed in Fig. 8. We suggest the generalization of the previous scheme in terms of algebraic multigrid theory.[27] This is an area of future research.

Sensitivity to Approximation Order and Emittance

All previous results have been based on the step spatial differencing scheme and the S_4 angular approximation. To investigate the sensitivity of the adaptive rebalance scheme to higher spatial and angular differencing orders, case 1 was reanalyzed using the diamond difference (DD) scheme and a variety of S_n approximation orders. Figure 9 displays the convergence history for a 20 × 20 grid and scattering coefficient of 10. Results with no acceleration are also included for reference. The convergence histories for the various approximation orders are nearly identical, indicating little sensitivity of the rebalance scheme to either spatial or angular differencing orders.

Lastly, the impact of surface emittance on convergence was studied using the case 1 geometry. Table 2 shows the results for a 20 × 20 grid with and without rebalance acceleration. Both iterations and total CPU time are listed. Solution convergence is poor without rebalance and worsens as emittance decreases. In contrast, excellent convergence is obtained for

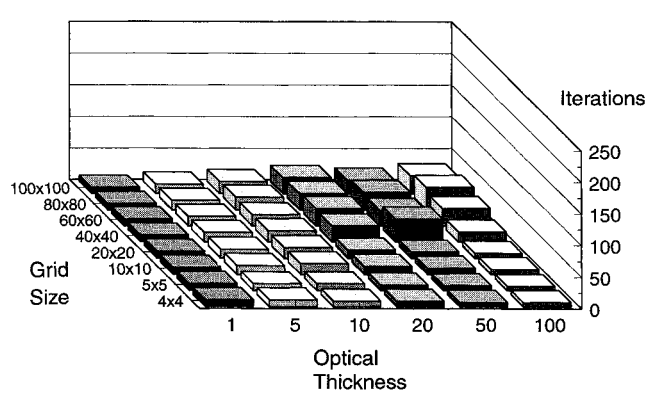

Fig. 8 Revised convergence of case 1 using adaptive rebalance method.

Table 2 Convergence and timing statistics for case 1 with and without adaptive rebalance (20 × 20 grid, $\sigma = 10$)

	No acceleration		With rebalance	
ε	Iterations	CPU time, s	Iterations	CPU time, s
0.1	804	23.89	31	1.32 (20%)[a]
0.3	351	10.30	21	0.85 (20)
0.5	247	7.37	18	0.72 (15)
0.7	201	5.96	17	0.68 (18)
0.85	180	5.38	17	0.65 (20)
1.0	166	4.89	17	0.64 (17)

[a]The value in parentheses denotes rebalance overhead, percent of total CPU time (with HP 9000/755 workstation) used to formulate and solve the rebalance equations.

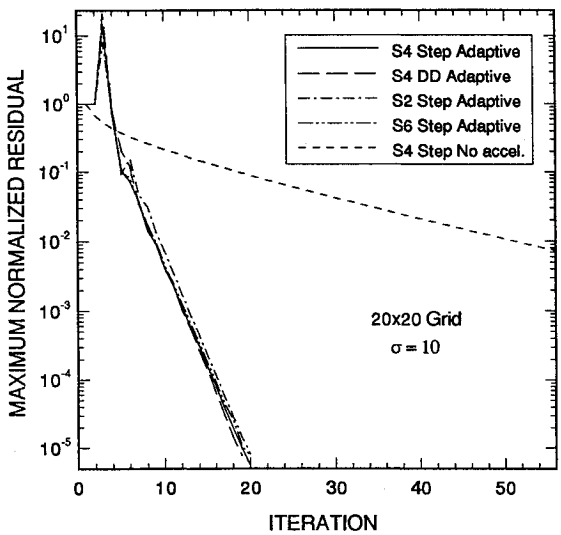

Fig. 9 Sensitivity of adaptive scheme to spatial and angular approximation order.

the full range of surface emittance when rebalance is applied. An order of magnitude improvement in iterations and CPU time is provided. In addition, the previous supposition of fractional overhead required by the rebalance scheme is validated (see values in parentheses in Table 2). These results indicate that the convergence characteristics of the rebalance scheme are generally insensitive to surface emittance when the acceleration method is consistently applied.

Conclusions

This article presents several acceleration schemes for the RTE, including successive overrelaxation, and synthetic acceleration and mesh rebalance methods. Solution convergence is discussed and demonstrated using simple examples in two and three dimensions. All methods show some degree of improved convergence. The mesh rebalance method is shown to converge best, but it fails to produce convergence of the RTE for large optical thicknesses and fine discretizations. Convergence can be dramatically improved by solving the rebalance equation on a coarser grid, which is determined by regrouping the base RTE grid until an optical thickness of near unity is obtained on the coarse grid. A general grouping strategy for property variations will be addressed in future work. Future research should also address use of the methods for nongray and anisotropic scattering applications.

References

[1]Viskanta, R., and Menguc, M. P., "Radiation Heat Transfer in Combustion Systems," *Progress in Energy and Combustion Science*, Vol. 13, No. 2, 1987, pp. 97–160.

[2]Modest, M. F., *Radiative Heat Transfer*, McGraw–Hill, New York, 1993.

[3]Fiveland, W. A., "Discrete-Ordinates Solutions of the Radiative Transport Equation for Rectangular Enclosures," *Journal of Heat Transfer*, Vol. 106, No. 4, 1984, pp. 699–706.

[4]Fiveland, W. A., "Three-Dimensional Radiative Heat Transfer Solutions by the Discrete-Ordinates Method," *Journal of Thermophysics and Heat Transfer*, Vol. 2, No. 4, 1988, pp. 309–316.

[5]Fiveland, W. A., "The Selection of Discrete Ordinate Quadrature Sets for Anisotropic Scattering," American Society of Mechanical Engineers HTD-Vol. 72, 1991, pp. 89–96.

[6]Truelove, J. S., "Discrete-Ordinates Solutions of the Radiation Transport Equation," *Journal of Heat Transfer*, Vol. 109, No. 4, 1988, pp. 1048–1051.

[7]Kim, T. K., and Lee, H., "Effect of Anisotropic Scattering on Radiative Heat Transfer in Two-Dimensional Rectangular Enclosures," *International Journal of Heat and Mass Transfer*, Vol. 31, No. 8, 1988, pp. 1711–1721.

[8]Jamaluddin, A. S., and Smith, P. J., "Predicting Radiative Transfer in Axisymmetric Cylindrical Enclosures Using the Discrete Ordinates Method," *Combustion Science and Technology*, Vol. 62, Nos. 4–6, 1988, pp. 173–186.

[9]Lewis, E. E., and Miller, W. F., *Computational Methods of Neutron Transport*, Wiley, New York, 1984.

[10]Fiveland, W. A., and Jamaluddin, A. S., "Three-Dimensional Spectral Radiative Heat Transfer Solutions by the Discrete Ordinates Method," *Journal of Thermophysics and Heat Transfer*, Vol. 5, No. 3, 1991, pp. 335–339.

[11]Chui, E. H., and Raithby, G. D., "Implicit Solution Scheme to Improve Convergence Rate in Radiative Transfer Problems," *Numerical Heat Transfer*, Pt. B, Vol. 22, 1992, pp. 251–272.

[12]Chandrasekhar, S., *Radiative Transfer*, Oxford Univ. Press, London, 1950.

[13]Lathrop, K. D., and Carlson, B. G., "Discrete Ordinates Angular Quadrature of the Neutron Transport Equation," Los Alamos Scientific Lab. Rept., LASL-3186, Los Alamos, NM, 1965.

[14]Raithby, G. D., and Chui, E. H., "A Finite-Volume Method for Predicting a Radiant Heat Transfer in Enclosures with Participating Media," *Journal of Heat Transfer*, Vol. 112, 1990, pp. 415–423.

[15]Chai, J. C., Lee, H. S., and Patankar, S. V., "Finite Volume Method for Radiation Heat Transfer," *Journal of Thermophysics and Heat Transfer*, Vol. 8, No. 3, 1994, pp. 419–425.

[16]Fiveland, W. A., and Jessee, J. P., "A Comparison of Discrete Ordinates Formulations for Radiative Heat Transfer in Multidimensional Geometries," *Journal of Thermophysics and Heat Transfer*, Vol. 9, No. 1, 1995, pp. 47–54.

[17]Varga, R. S., *Matrix Iterative Analysis*, Prentice–Hall, Englewood Cliffs, NJ, 1962.

[18]Wachspress, E. L., *Iterative Solution of Elliptic Systems and Applications to the Neutron Diffusion Equations of Reactor Physics*, Prentice–Hall, Englewood Cliffs, NJ, 1966.

[19]Reed, W. H., "The Effectiveness of Acceleration Techniques for Iterative Methods in Transport Theory," *Nuclear Science and Engineering*, Vol. 45, No. 3, 1971, pp. 245–254.

[20]Alcouffe, R. E., "Diffusion Synthetic Acceleration Methods for the Diamond-Differenced Discrete-Ordinates Equations," *Nuclear Science and Engineering*, Vol. 64, No. 2, 1977, pp. 344–355.

[21]Ratzel, A. C., and Howell, J., "Two Dimensional Radiation in Absorbing-Emitting-Scattering Media Using the P-N Approximation," *Journal of Heat Transfer*, Vol. 105, No. 2, 1983, pp. 333–340.

[22]Van Dyke, M., *Perturbation Methods in Fluid Mechanics*, The Parabolic Press, Stanford, CA, 1975.

[23]Brandt, A., "A Multi-Level Adaptive Solution of Boundary Value Problems," *Mathematics of Computation*, Vol. 31, No. 138, 1977, pp. 333–390.

[24]McCormick, S., *Multigrid Methods*, Vol. 3, SIAM Frontiers Series, Society for Industrial and Applied Mathematics, Philadelphia, PA, 1987.

[25]Briggs, W. L., *A Multigrid Tutorial*, Society for Industrial and Applied Mathematics, Philadelphia, PA, 1987.

[26]Hackbusch, W., and Trottenberg, U., *Multigrid Methods*, Springer–Verlag, Berlin, 1982.

[27]Ruge, J. W., and Stüben, K., "Algebraic Multigrid," *Multigrid Methods*, edited by S. McCormick, Vol. 3, SIAM Frontiers Series, Society for Industrial and Applied Mathematics, Philadelphia, PA, 1987.